Solar Energy Materials & Solar Cells 218 (2020) 110752

Contents lists available at ScienceDirect

Solar Energy Materials and Solar Cells

journal homepage: http://www.elsevier.com/locate/solmat

Investigation of light-induced degradation in N-Type silicon heterojunction solar cells during illuminated annealing at elevated temperatures

Chukwuka Madumelu [1], Brendan Wright [1], Anastasia Soeriyadi, Matthew Wright, Daniel Chen, Bram Hoex, Brett Hallam [*]

School of Photovoltaic and Renewable Energy Engineering, UNSW Sydney, Australia

ARTICLE INFO

Keywords:
Light-induced degradation (LID)
Silicon heterojunction (SHJ)
Hydrogen
Stability
Surface passivation

ABSTRACT

In this paper, we study a light-induced degradation (LID) mechanism observed in commercial n-type silicon heterojunction (SHJ) solar cells at elevated temperatures using dark- and illuminated annealing for a broad range of illumination intensities (1–40 kWm^{-2}) at temperatures from 25 to 180 °C. Three key results are identified. Firstly, an increase in solar conversion efficiency (η) of up to 0.3% absolute is observed after 3 min of dark annealing at 160 °C, attributed to improved surface passivation and a reduction in series resistance. Secondly, a temperature-dependent light-induced degradation behaviour is observed at temperatures as low as 85 °C under 1-sun equivalent illumination, with increasing degradation extent and rate for increasing temperatures. At 160 °C, an average η loss of 0.5 ± 0.3% absolute is observed after only 5 min and exceeding 0.8% in some cells. Thirdly, a subsequent light intensity-dependent recovery occurs with continued illumination exposure. Under 1-sun illumination at 160 °C, a reduction in net η loss up to 0.05 ± 0.1% absolute is observed after 2 h. Increasing the illumination intensity to 40 kWm^{-2} accelerates the recovery and can result in a net η improvement of 0.2% absolute at 150 °C within 100 s. The results suggest that attempts to improve the efficiency of SHJ solar cells using illuminated annealing could be detrimental to cell performance if not carefully optimised. Further investigation is required to identify the exact nature of the underlying defect mechanism(s) and develop appropriate mitigation strategies on commercially suitable timescales.

1. Introduction

The superior silicon interface passivation provided by thin hydrogenated amorphous silicon (a-Si:H) layers typically employed in passivating contacts in silicon heterojunction (SHJ) solar cells has been instrumental to the success of this architecture. This is evident from the high open-circuit voltage (V_{OC}) of 750 mV [1] measured on record SHJ solar cells, and the current world record solar conversion efficiency (η) of 26.7% for a back contact SHJ device [2]. Due to the excellent V_{OC} achieved on SHJs, they have very low temperature coefficients [3–5], making them attractive for deployment in high-temperature climates. Additionally, SHJ cells are perceived to have a reduced susceptibility to light-induced degradation (LID) [6], the most widely studied degradation mechanism in solar cells, and thus experience lower relative power losses during long-term operation in-field.

With numerous advantages, the long-term outlook for this technology appears very positive, as is indicated by a projected three-fold increase in market share from about 5% to 15% within a decade, as well as the n-type Czochralski (Cz) silicon wafers (n-c-Si) on which they are based, projected to increase from the current 15% to about 45% market share over the same period [7]. A successful increase in SHJ uptake will depend largely upon the ability of the cells to maintain the excellent surface passivation - instrumental to their high efficiencies - over the lifetime of the panels. Thus, it is imperative that the long-term stability of SHJs is properly understood, and potential power loss mechanisms are identified and mitigated.

Presently, there exists limited knowledge and even conflicting reports regarding the long-term stability of SHJs during in-field operation. Indeed, there exist numerous reports suggesting the possibility of degradation in performance under illumination. A comprehensive study by Jordan et al. showed unexpectedly high degradation in some field-mounted SHJ modules, dominated by V_{OC} losses and an increase in

* Corresponding author.
E-mail address: brett.hallam@unsw.edu.au (B. Hallam).
[1] equal authorship contribution.

https://doi.org/10.1016/j.solmat.2020.110752
Received 31 May 2020; Received in revised form 20 July 2020; Accepted 17 August 2020
Available online 1 September 2020

series resistance (R_S); up to a 50% reduction in the minority charge carrier lifetime was observed [8]. The reduction in performance was also found to be uniform across all cells within a module, implying a similar mechanism responsible for the observed degradation. Sharma et al. reported a peak power decay per year of 0.36% in SHJ modules after 28 months of observation. Their analysis indicated that while V_{OC} increased by 9%, the majority of observed losses were due to a 14% decay in fill factor (FF), attributed to an increase in R_S and/or a decrease in shunt resistance (R_{Sh}) [9]. Karas et al. Observed degradation in Cu-plated SHJ cells and modules due to losses in V_{OC}, short-circuit current (J_{SC}), and FF after damp heat testing [10]. They noted that the onset of loss in surface passivation, responsible for the observed V_{OC} loss, occurred slower than that of either J_{SC} and FF. Krajangsang et al. reported a degradation in η which was primarily attributed to a 5% reduction in J_{SC} for a SHJ cell with a p-type micro-crystalline (μc-Si:H) emitter [11].

While these reports indicate the potential for LID in SHJ cells, Koboyashi et al. reported a 0.3% absolute increase in η after light soaking at 30 °C under 1-sun illumination for both cells and modules. They attributed this increase to improvement in surface passivation resulting in an increase in both V_{OC} and FF [12]. They noted that the improvement was similarly observed with carrier injection under forward bias (without illumination), and was not dependent on the illumination intensity. It should be noted, however, that some of the previous studies conducted showing degradation involved 10+ year-old field-mounted modules, and have been criticized for the fact that they contained legacy SHJ technology which is not representative of current state-of-the-art production [13].

The effect of light soaking on SHJ cell precursors featuring thin a-Si:H layers has been intensively studied. Various authors have shown a significant increase in defect density at both the hetero-interface and the a-Si:H bulk with increasing light soak time [14–16] and attributed this to the Staebler-Wronski effect (SWE) [17–20]. This effect, which is observed in a-Si:H under extended and intense illumination, is thought to be caused by the formation of electronically-active silicon dangling-bond defects. Although the exact mechanism of the SWE is not yet fully understood, the role of hydrogen in the metastable defect formation is agreed upon by most researchers. It is thought that the exchange of hydrogen atoms facilitates the formation of molecular H_2, resulting in a de-passivation of dangling bonds within the bulk of the a-Si, or that the density of weak Si–Si bonds increases in regions with clustered hydrogen atoms [21–23].

More recently, in conventional p-type silicon solar cells, a new LID mechanism called light- and elevated temperature-induced degradation (LeTID) was identified, capable of causing a loss in η of up to 16% relative in multi-crystalline silicon cells under illumination [24–27]. However, it has subsequently been shown to affect both p-type and n-type Cz materials [28], and even float-zone silicon [29]. It has been suggested that hydrogen may play an important role both in the defect formation [30–32], and additionally as a mitigation agent [33]. The high-temperature metal contact firing step has been found to be key in activating the defect [34–36]. This is due to the release of hydrogen from the hydrogenated dielectric layers, and the subsequent distribution of the atomic hydrogen throughout the bulk. This then enables degradation during subsequent light-soaking, although there is some evidence that this degradation can occur even without a firing step [37]. While SHJ cells do not undergo the high temperature firing step, they do feature H-rich selective contact layer stacks (a-Si:H) making them also potentially susceptible to LeTID, as a significant amount of hydrogen could enter the silicon bulk during the thin film deposition and subsequent curing of the metal contacts at temperatures in the vicinity of 200 °C. Recent publications have shown effective passivation of boron-oxygen defects in boron-doped p-type SHJ solar cells and n-type upgraded metallurgical grade Cz silicon co-doped with boron and phosphorus, without a dedicated prior high-temperature process [38,39]. This indicates that the SHJ solar cell fabrication process could also provide sufficient hydrogen to cause hydrogen-related degradation in the n-type Cz silicon bulk.

The widely varied and conflicting reports in the literature for SHJ solar cells, with some reported losses in SHJ cell power (η, V_{OC}, J_{SC}, FF) under illumination, while others have reported performance-related improvements under comparable conditions, highlights the need for further investigations into the long-term stability and reliability of power generation for state-of-the-art SHJ cells. In particular, a detailed understanding is sorely needed of the underlying causal mechanisms of these instabilities, and exactly how they are influenced by differences in SHJ cell architecture. In this study we present an investigation into the response of state-of-the-art SHJ solar cells to illuminated annealing at elevated temperatures.

Firstly, we present *ex-situ* current-voltage (I–V) measurements for cells processed exposed to dark or illuminated annealing at 160 °C, complimented by *in-situ* V_{OC} measurements at a range of annealing temperatures. Second, we present accelerated degradation results performed using an automated tool with a high degree of precision and control in each of: temperature, illumination intensity, and exposure time; ideal for the study of both kinetics and extent of degradation and recovery behaviour exhibited by these SHJ cells. Additionally, this equipment facilitated illumination power densities up to 40 kWm^{-2}, with instant on/off capability, all while maintaining a spatially uniform illumination area over the entire surface of the 6 inch cells. Through these results, we demonstrate that LID is observed in SHJ cells, which has both a temperature and illumination intensity dependence, and can lead to a loss in η of up to 0.8% absolute.

2. Experimental methods

2.1. Cell architecture

Commercially sourced front-junction n-type SHJ cells (6 inch, bifacial) were obtained for this study, with measured average V_{OC} and η of 728 ± 3 mV and 21.8 ± 0.2% respectively. The structure of these cells (see Fig. 1) featured an n-type mono-crystalline (Cz) silicon wafer, with selective contact stacks at each interface comprising: a thin intrinsic a-Si:H passivation layer and doped (p/n) a-Si:H carrier selective layers, capped with indium-tin oxide (ITO) films and plated metal (Cu and Sn) contacts. A reasonable grouping was observed for the initial V_{OC} of all processed cells across illuminated annealing, *in-situ* V_{OC}, and accelerated degradation experiments, with variance ranges within 5.0 mV, 0.5%, and 0.5% absolute for V_{OC}, pFF, and η respectively. Five identical cells were processed for each set of conditions to ensure statistical significance of results.

2.2. Illuminated annealing

To investigate the LID dynamics, the SHJ cells were split into two main groups: (Group 1) dark-annealed (DA) on a hotplate at 160 °C; (Group 2) light-soaked (LS) on a hotplate with illumination (four broadband halogen lamps calibrated to 1 kWm^{-2} using a ThorLabs PM100D power meter); both groups at a temperature of 160 °C. Verification of the actual cell temperature was performed using a digital multimeter with K-type thermocouples. Additionally, a control cell was obtained from the same batch and was used as a reference for all experiments, measured at each increment of exposure time without undergoing processing to account for any fluctuations during intermittent current-voltage (I–V) measurements.

2.3. In-situ open-circuit photovoltage

Using a custom voltage probe station, *in-situ* V_{OC} measurements were carried out on a group of cells from the same batch as used for the illuminated annealing studies, performed using a 1 kWm^{-2} power density (identical light source as in illuminated annealing experiments) at temperatures between 85 °C and 180 °C. In this set-up, the hot plate

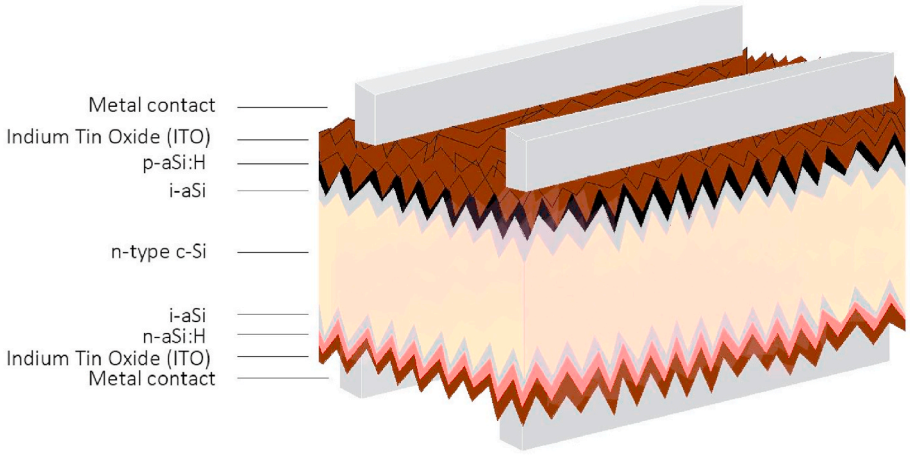

Fig. 1. An architectural schematic of the silicon heterojunction solar cells investigated herein. (For interpretation of the references to colour in this figure legend, the reader is referred to the Web version of this article.)

stage on which the cell was mounted served as the rear contact, while a second voltage probe pin was placed on one of the busbars on the front surface of the cell. The set-up was equipped with a data logger, and a data acquisition rate of 10 samples per second was used to measure the V_{OC}.

2.4. Accelerated degradation

For accelerated degradation testing, cells were exposed to temperatures (25–180 °C) and illumination (5–40 kWm^{-2}) using a commercial tool (DR Laser Tech. Corp. Ltd.). The cell temperature was controlled during processing via a hotplate (with integrated vacuum for good thermal contact) with a stable temperature range from 25 °C to over 300 °C. The thermal set-point was regulated via a feedback circuit and compressed air-cooling system, incorporating an IR thermal sensor for cell surface temperature measurement. Automated loading and unloading of cells to and from the processing stage was achieved with computer-controlled vacuum arm, enabling precision in processing times on the order of 0.2 s. Controllable illumination was achieved using a 980 nm continuous-wave laser with up to 155 kWm^{-2} power density range capability with uniform illumination over a 200 mm × 200 mm area. Rapid cell cooling was achieved via compressed air knives directly after removal from the hotplate. Additionally, to establish any impact of thermal cycling on cell dynamics during the standard *ex-situ* processing and characterisation procedures, validation tests were performed to compare iterative processing up to 30 s in 5 s increments, versus a single 30 s process. The results exhibited no significant difference in cell performance changes between the two processing approaches.

2.5. Current-voltage characterisation

For all *ex-situ* studies, after each increment of exposure time, the cells were removed from the illuminated annealing set-up and allowed to cool down to room temperature for calibrated I–V measurements using a commercial solar simulator (LOANA by pv-tools GmbH); each cell was affixed via vacuum to a temperature-controlled chuck at 25 °C during reverse/forward bias current-voltage sweep under standard testing conditions (AM1.5G, 1 kWm^{-2}). In addition to a standard I–V sweep, a Suns-Voc measurement was also performed to obtain an I–V response without the influence of series resistance (R_S), and thereby calculate pseudo fill factor (pFF). The R_S was obtained by comparing the Suns-Voc curve with the 1-sun I–V response at the maximum power point [40].

2.6. Illumination sources

Although the light sources were carefully calibrated to have an equivalent power density comparable to AM1.5 solar irradiance (1kWm^{-2}), there exist significant difference in the spectrum of each (single wavelength excluding UV or IR, halogen with additional IR, broadband LEDs), as compared to the solar spectrum, which may lead to different in-field results from those presented in this paper. For consistency we have used illumination power density to normalise and make comparison to equivalent solar irradiance where necessary. Critically, light-induced degradation observed under broadband halogen lamp illumination would indicate that the solar spectrum is likely to have a similar effect.

3. Results and discussion

3.1. Impact of dark and 1-sun illuminated annealing at 160 °C

To investigate the stability of SHJ cells, two groups of cells, each comprising five randomly selected cells, underwent exposure to either dark-annealing (DA, Group 1) or light-soaking (LS, Group 2) with 1 kWm^{-2} illumination intensity at 160 °C. These cells exhibited an average initial η and V_{OC} of 21.9 ± 0.1% and 728 ± 3 mV, respectively. A reference cell (Ref) was measured in parallel, exposed to neither heat nor illumination. The I–V characteristics of the individual cells were measured *ex-situ* at regular intervals. The results of η change for individual cells in each group as a function of exposure time are displayed in Fig. 2, to clearly highlight the variability in the response of individual cells. The complete results for cell performance variation for Groups 1 and 2 at 1 kWm^{-2} illumination intensity, all at 160 °C, are displayed in Fig. 3 as box plots. Each plot includes individual cell response values (circles), box plots indicating mean and standard deviation of each five-cell group, and the time-averaged group behaviour over exposure time (broken line) to guide the eye.

All measurements of the reference cell were ±0.05% in absolute efficiency throughout the experiment, indicating stable I–V measurements and that changes in other groups were, indeed, caused by processing rather than errors in IV measurements. It is immediately obvious from the results displayed in Fig. 2 that there is a stark difference in η variation between Group 1 (DA) and Group 2 (LS) cells. While Group 1 cells showed an average efficiency improvement of 0.2 ± 0.1% absolute after 10 min of DA, and which remained comparatively stable up to 1 h, the addition of illumination resulted in a sharp reduction in η, an average of 0.5 ± 0.3% absolute within 5 min, with a maximum degradation of 0.8% absolute. Further, a subsequent recovery is observed for all cells,

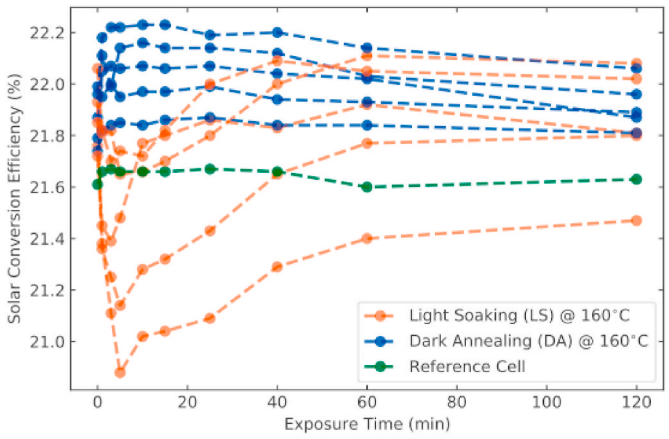

Fig. 2. Solar conversion efficiency of individual cells (points with broken line to guide the eye) as a function of time after either dark-annealing (DA) or light-soaking (LS) at 1 kWm^{-2} illumination intensity (broadband halogen), both at a temperature of 160 °C. A reference cell (Ref) is included, exposed to neither heat or illumination and stored in the dark at room temperature between measurements. All I–V measurements were conducted ex-situ under standard testing conditions.

plateauing at a value comparable to that of the initial pre-exposure η within 1 h in some cases. Interestingly, the J_{SC} is observed to be effectively stable for both DA and LS conditions, with maximum variation of ~0.1 ± 0.05 $mAcm^{-2}$.

Additionally, although all cells were produced at the same production line and were taken from the same efficiency bin, the individual cells show a quite significant variability. In the individual Group 1 cells for example (Fig. 2), η remained virtually unchanged for some cells after 10 min of DA, while others improved by ~0.3% absolute. Likewise, in Group 2 the loss in η ranged from 0.1 to 0.8% absolute after 5 min of LS. While arising primarily from changes in V_{OC} and pFF, the origin of this cell-to-cell variation is currently not known and requires further investigation.

For the DA group, an average increase in η of 0.2% absolute was observed within the first 5 min, appearing relatively stable beyond this point, and looks to arise from a combination of both V_{OC} and pFF with average increases of 2 mV and 0.5% absolute, respectively. A reduction in R_S on the order of 0.05 Ωcm^{-2} was also observed and is comparable to that observed for the LS group, and therefore the changes in R_S appear independent of illumination.

Interestingly, the DA condition which facilitates the observed improvement is similar to that generally used for curing SHJ cells after production. It is possible that the observed gain was also present directly after production but has since reduced, possibly indicating a metastable state under standard storage conditions which is re-activated after the DA process. Another possibility is that the post-production curing step was not sufficient to completely achieve the potential improvements, and hence the further improvement observed after 10 min of DA. However the existence, if any, of such a metastable state requires further investigation, and would present two implications: (1) that the gains herein observed are also unstable; (2) the gains may not be present in the field if optimal conditions to activate it are not met. It is noteworthy to mention that the process of module fabrication may confer similar enhancements to those observed during DA, since the process is undertaken in similar conditions.

Illuminated annealing (1-sun equivalent, 160 °C) leads to a remarkable degradation of solar cell performance, in sharp contrast to the cells annealed in the dark. The LS group exhibits a strong initial degradation up to maximum extent at 5 min, with reductions in V_{OC} and pFF as high as 13 mV and 2.0% absolute, respectively, yielding a peak loss in η from 21.8% down to 21.0%. This is followed by a recovery phase that begins to stabilize beyond 2 h, and while the V_{OC} was observed to completely recover, even exceeding the initial value by an average of 3 mV, the pFF did not exhibit a complete recovery and remained 0.5% absolute below the pre-processed state.

While annealing in the dark for a short time may be beneficial and lead to slight improvements in cell performance, it is obvious that illuminated annealing can lead to significant degradation and can potentially result in irreversible losses in power generation. The loss of both V_{OC} and pFF at the point of maximum degradation during LS may indicate a reduction in effective minority carrier lifetime, arising from an increase in bulk or surface recombination-active defects [41], however this requires further investigation.

Fitting of each cell I–V response using a simple 2-diode equivalent-circuit model provided the two diode saturation-current densities, J_{01} and J_{02}, which represent the recombination contributions from the passivated contact interface, and regions of the cell not limited by the minority charge carrier density, respectively. The resulting J_{01} and J_{02} values obtained for both DA and LS groups (as presented in Fig. 3) are displayed in Fig. 4. The DA group show an average 30% reduction in J_{01} within 5 min, while J_{02} is effectively stable to beyond 2 h. These results support the suggestion of improved surface passivation due to lower interface recombination and is consistent with the observed improvement in both V_{OC} and pFF (and consequently η) presented in Fig. 3.

With the addition of illumination, however, J_{01} increases by over 80% within the first 3 min of exposure, before recovering back to below the initial state after 2 h, closely mirroring the behaviour observed in V_{OC} change. A smaller change is observed to occur in J_{02}, with an average maximum increase of 44% after 5 min. Beyond this point J_{02} decreases, however, does not completely recover within 2 h, and more closely resembles the behaviour observed in pFF. Interestingly, while the values of J_{01} after 2 h LS exhibit average and standard deviation close to that of the initial state, the standard deviation at the extent of maximum degradation is almost 3 times higher, again highlighting the high cell-to-cell variability.

3.2. *Impact of temperature and illumination intensity*

As the changes in V_{OC} appeared to dominate the primary LID behaviour observed for these cells during illuminated annealing, *in-situ* photovoltage measurements were used to directly monitor changes in cell V_{OC} during LS at a range of elevated temperatures. The resulting ΔV_{OC} values (relative to initial V_{OC}) were temperature-corrected to room-temperature using a temperature coefficient of 2.07 mV $^{\circ}C^{-1}$ (experimentally determined using identical cells to those used throughout this study), and are presented in Fig. 5.

Both the time and extent of maximum V_{OC} degradation were observed to accelerate with increasing cell temperature. In particular, a large reduction in the kinetics and extent of both the degradation and subsequent recovery was observed for temperatures below 120 °C. The time at maximum degradation extent for the transients above 120 °C is on the order of 200 s, while the cells annealed at 85 °C and 100 °C took up to 3 h to reach their maximum level of degradation. However, due to the inherent temperature sensitivity of *in-situ* V_{OC} monitoring, and the high degree of cell-to-cell variation already observed, these individual transients alone do not provide sufficient confidence regarding the temperature dependence of the LID behaviour. As such, more extensive *ex-situ* studies were performed to validate these results and are presented in the following section.

It is interesting to note that the 5 ± 3 mV V_{OC} improvement at long illuminated annealing times is comparable to that reported by Kobayashi et al. [12], that of a 4 mV improvement and corresponding 0.3% absolute η improvement, both under illumination and via current injection, at elevated temperatures up to 75 °C. It also appears that a comparable net V_{OC} improvement is obtained at all measured annealing temperatures, however the time to final V_{OC} improvement is significantly accelerated at higher temperatures, by over an order of magnitude from 85 °C up to 160 °C.

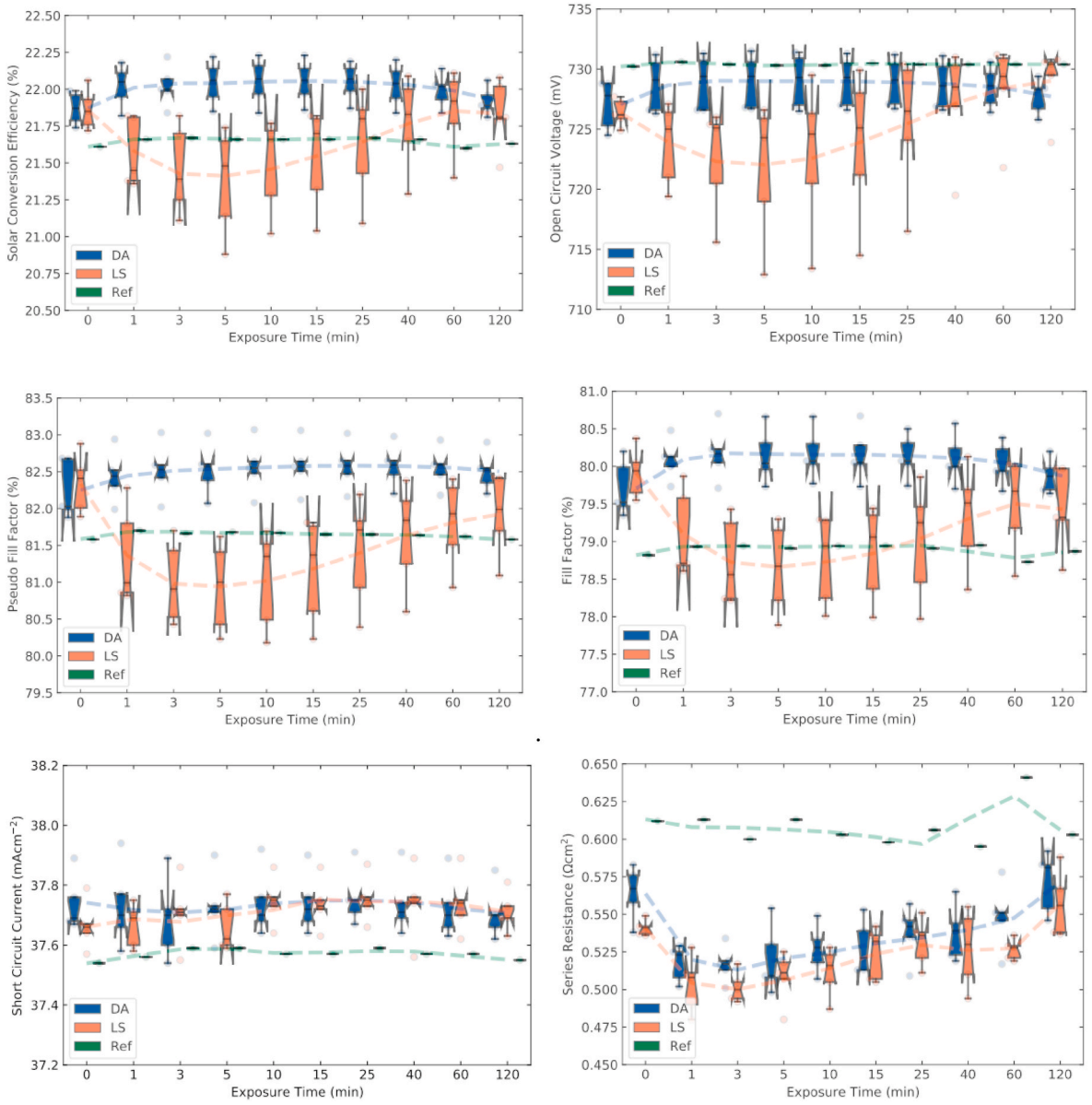

Fig. 3. Cell performance as a function of post-processing time after either dark-annealing (DA) or light-soaking (LS) at 1 kWm^{-2} illumination intensity (broadband halogen) at a temperature of 160 °C. A reference cell (Ref) is included, exposed to neither heat or illumination. Displayed are solar conversion efficiency (top left), open-circuit voltage (top right), pseudo fill factor (middle left), fill factor (middle right), short-circuit current (bottom left), and series resistance (bottom right); each plot includes individual cell response values (circles), box plots indicating mean and standard deviation of each five-cell group, and the time-averaged group behaviour over exposure time (broken line) to guide the eye. All I–V measurements were conducted ex-situ under standard testing conditions.

The elevated temperature light-soaking (Figs. 2–4) and *in-situ* open-circuit photovoltage (Fig. 5) results strongly indicate the existence of a temperature-dependent, light-induced degradation mechanism. As such, the following section presents results detailing the kinetics and extent of both degradation and recovery behaviours, as well as its dependence on cell temperature and illumination intensity, monitored through changes in V_{OC} as a function of exposure time relative to initial pre-exposure values. For each combination of temperature and illumination intensity, five equivalent cells were incrementally exposed for up to an aggregate 100 s, with *ex-situ* I–V measurements (room temperature, AM1.5) performed at each time step.

As previously stated, the J_{SC} variation was found to be insignificant within the investigated temperature and illumination intensity range. Further, the kinetics and extent of variation in pFF during exposure effectively mirror those observed for V_{OC}, but with some additional degradation yielding a lesser extent of recovery. It was therefore decided that presenting results for V_{OC} alone was sufficient to characterize the dynamics of this light-induced defect mechanism. Given that bulk degradation in p-type Cz and p-type multi-crystalline silicon solar cells caused by B–O LID and LeTID results in a significant reduction in the J_{SC} [42,43], while no significant change in J_{SC} is observed in the presented results, degradation within the heterointerface may represent the primary mechanism, rather than a bulk defect in n-type Cz. However, as shown in simulation results by Steinkemper et al. [44], bulk recombination without significant losses in V_{OC} is possible in SHJ cells without a change in J_{SC}. Further investigations are therefore required to better understand the recombination mechanisms underlying the observed degradation and recovery behaviour.

The analysis and interpretation of cell dynamics presented herein utilized the average behaviour of each cell group, rather than individual cell responses, in order to simplify the additional complexity of the observed cell-to-cell variability as already discussed (differences in

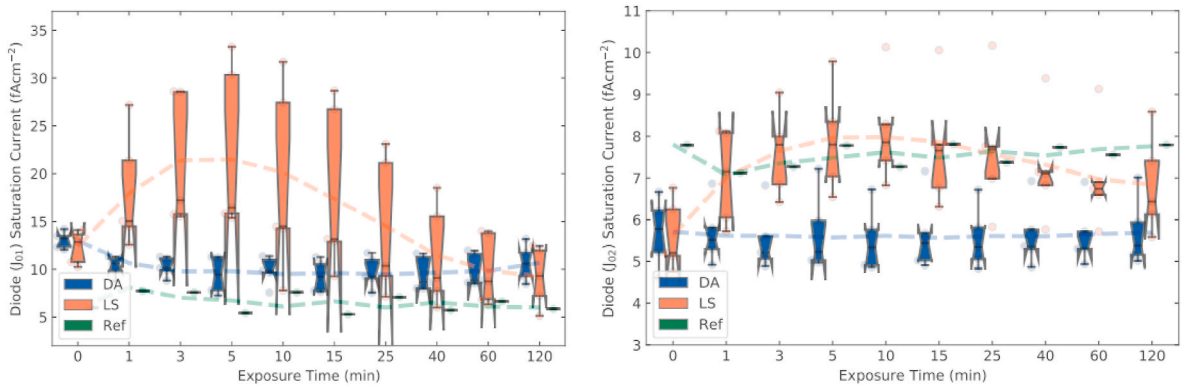

Fig. 4. Cell performance as a function of post-processing time after dark-annealing (DA) or light-soaking (LS) at a 1 kWm^{-2} illumination intensity at a temperature of 160 °C. A reference cell (Ref) is included, exposed to neither heat or illumination. Displayed are diode saturation-current densities J_{01} (left) and J_{02} (right) obtained from fitting to a 2-diode equivalent circuit model; each plot includes individual cell response values (circles), box plots indicating mean and standard deviation of each five-cell group, and time-averaged group behaviour over exposure time (broken line). All I–V measurements were conducted ex-situ under standard testing conditions.

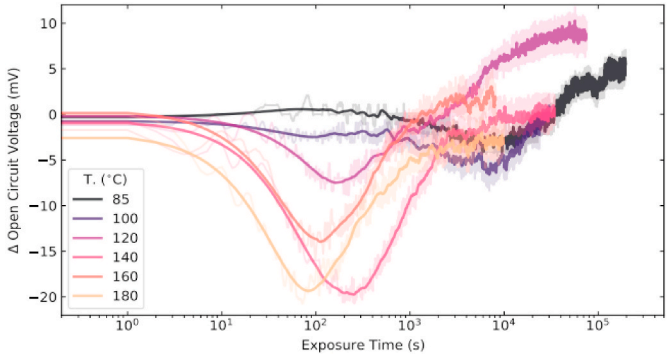

Fig. 5. In-situ differential open-circuit photovoltage as a function of time for cells annealed at temperatures from 85 °C to 180 °C under 1 kWm^{-2} illumination intensity (broadband halogen).

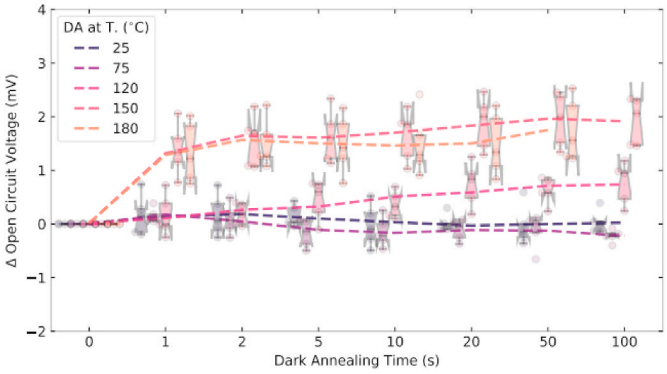

Fig. 6. Cell open-circuit voltage as a function of time after exposure to a range of elevated temperatures (as labelled) without illumination: individual cell response values (circles), box plots indicating mean and standard deviation of each five-cell group, and time-averaged transient over exposure time (broken line) to guide the eye. All I–V measurements were conducted ex-situ under standard testing conditions.

behaviour between apparently identical cells). The average trends in V_{OC} regarding the degradation/recovery kinetics and extent do, however, still accurately capture the qualitative behaviour of the identified defect, as well as its dependence on both temperature and illumination intensity. More advanced modelling methods are required to extract additional detail from individual cell behavioural variations, and this is left to future work.

Firstly, dark annealing (no illumination) of the SHJ cells was performed at a range of temperatures. Fig. 6 shows the change in V_{OC} relative to the initial (ΔV_{OC}) after exposure to a range of temperatures (as labelled) without illumination. Both the 25 °C and 75 °C groups exhibit no ΔV_{OC} within the measured exposure time. The 120 °C group exhibits a gradual increase in ΔV_{OC}, up to 1 mV after 100 s exposure time. Both 150 °C and 180 °C groups exhibit comparable rapid increases in ΔV_{OC}, up to 2 mV within 2 s exposure time, followed by a stable plateau beyond. This improvement in V_{OC} is comparable to that observed in the previously presented dark-annealing results (Fig. 3, top right) at a temperature of 160 °C. Based on the qualitative differences observed between groups, a temperature on the order of 120 °C appears to represent a threshold between two distinct behaviours within the time frame of these experiments, that of no ΔV_{OC} for temperatures below, and effectively instantaneous increase to a maximum for temperatures above.

The addition of illumination produces both degradation and recovery of V_{OC}, similar to that observed in the previously presented light-soaking results (Fig. 3, top right). Fig. 7 exhibits the ΔV_{OC} after exposure to a range of elevated temperatures (as labelled) with a 40 kWm^{-2}

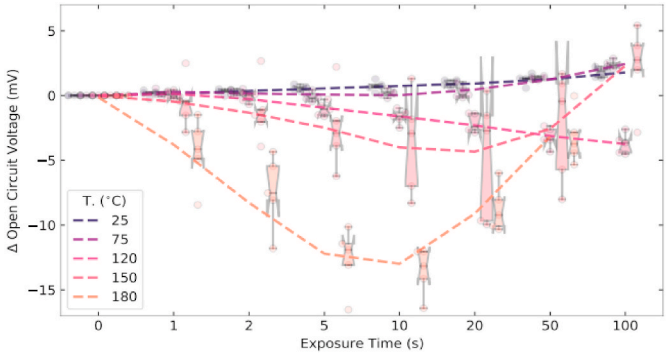

Fig. 7. Cell open-circuit voltage as a function of processing time after exposure to a range of elevated temperatures (as labelled) with an illumination intensity of 40 kWm^{-2} (single wavelength, 980 nm): individual cell response values (circles), box plots indicating mean and standard deviation of each five-cell group, and time-averaged transient over exposure time (broken line) to guide the eye. All I–V measurements were conducted ex-situ under standard testing conditions.

illumination intensity. Note the difference in ΔV_{OC} axis scale from that used in Fig. 6. These cell groups do however exhibit important differences from those observed under 1 sun illumination at 160 °C, primarily the kinetics of the degradation, and even more prominently the recovery appears significantly accelerated. The 150 °C group exhibits a maximum ΔV_{OC} degradation extent of 4 mV after 20 s exposure, compared to a 10 mV reduction after 240 s at a 160 °C cell temperature. These results were however obtained with a 40-fold greater illumination intensity, implying a strong influence of illumination intensity on the kinetics and extent of degradation and recovery, and will be discussed further below.

Looking now to the temperature dependence of ΔV_{OC} under a high illumination intensity, a clear increase in the kinetics of the initial degradation phase was observed with increasing temperature. The maximum ΔV_{OC} degradation extent of the 180 °C group, 13 mV at 10 s exposure time, is three times higher than the degradation observed at 150 °C, and also occurs in half the exposure time. However, further inspection of the lower temperature groups indicated additional complexity, with neither 25 °C or 75 °C groups exhibiting significant degradation, similar to the behaviour observed without illumination. Interestingly, although still trending towards further degradation beyond the longest measured exposure time of 100 s, the measurements taken at 120 °C and 150 °C exhibit comparable maximum ΔV_{OC} degradation extent. The 120 °C group does, however, exhibit slower degradation kinetics, in line with the trend at higher cell temperatures.

From these results it appears clear that the maximum extent of ΔV_{OC} degradation is influenced by an interdependent combination of temperature and illumination intensity. Additionally, temperatures below 120 °C do not exhibit behaviour distinct from that without illumination, again suggesting the existence of an effective thermal activation threshold modulating the expression of this light-induced degradation behaviour.

A final interesting observation from the results presented in Fig. 7 is that exposure to a 40 kWm^{-2} illumination intensity at 150 °C for 100 s is sufficient to more than completely recover the initial degradation in V_{OC}, yielding a 0.2% absolute improvement in η, albeit comparable to results obtained simply through dark annealing at the same elevated temperature. Dark-annealing, however does not result in the activation and mitigation of the primary light-induced defect, and therefore leaves commercial cells at risk of possible future performance losses due to degradation via accidental or incidental exposure to illumination at sufficiently elevated temperatures. Deliberate post-processing of SHJ cells with a combination of illumination and elevated temperatures may completely mitigate the impacts of this defect, as indicated by the results presented. Further studies are required to investigate the long-term stability of SHJ cells after deliberate post-processing, in order to validate whether these improvements are stable under extended in-field operation.

In order to investigate the illumination intensity dependence of the observed light-induced defect, cells were exposed to illumination intensities up to 40 kWm^{-2}. Fig. 8 exhibits ΔV_{OC} during exposure to illumination intensities (including without illumination) at a temperature of 150 °C. Interestingly, all cell groups were effectively equivalent up to 20 s of post-processing, with ΔV_{OC} steadily decreasing by 5.0 ± 2.0 mV. The initial degradation phase kinetics therefore appear independent of illumination intensity. However, beyond 20 s these three groups diverge: a continued decrease in ΔV_{OC} for the 5 kWm^{-2} group to a 13.0 ± 1.0 mV reduction at 100 s, while both 23 kWm^{-2} and 40 kWm^{-2} groups exhibit a recovery in ΔV_{OC}; the highest illumination intensity of 40 kWm^{-2} exhibits the fastest recovery phase kinetics, with the final ΔV_{OC} of 2.5 ± 1.0 mV exceeding both the initial value, and that observed without illumination (dark-annealing). These results indicate that increasing illumination intensity has the effect of accelerating the recovery kinetics at a given temperature, without noticeably influencing the kinetics of the initial degradation phase.

While the mechanisms underlying this thermally-activated, light-induced defect in n-type SHJ cells remain uncertain, the above results provide some insight through the dependence of degradation and recovery kinetics on temperature and illumination intensity. SWE type defect recovery could account for the temperature-dependent rise above the apparent threshold cell temperature of 120 °C, where thermally activated hydrogen-silicon defect mobility within the a-Si:H layer above ~100 °C may lead to the effusion of hydrogen, or lead to significantly altered interfacial passivation quality. This mechanism has been observed in several studies on a-Si/n-c-Si structures similar to those used within the investigated cells [12,22,45–49]. It is however clear that further investigations into the causal mechanism(s) of the observed LID behaviour are required to better understand the primary factors influencing defect activation, and both the kinetics and extent of degradation and recovery, as well as thorough investigation using more field-relevant testing conditions.

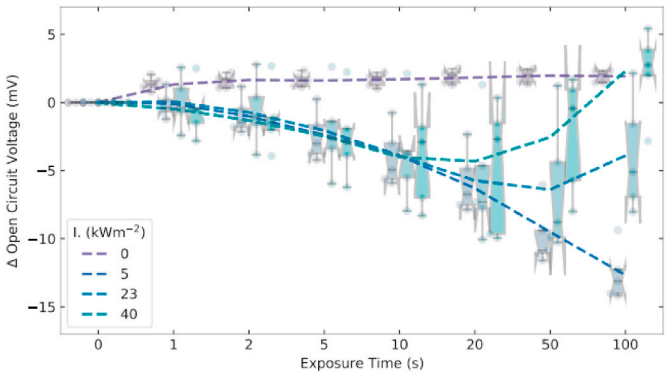

Fig. 8. Cell open-circuit voltage as a function of time after exposure to a range of illumination intensities (as labelled; single wavelength, 980 nm) at a temperature of 150 °C: individual cell response values (circles), box plots indicating mean and standard deviation of each five-cell group, and time-averaged transient over exposure time (broken line) to guide the eye. All I–V measurements were conducted ex-situ under standard testing conditions.

4. Conclusions

In this paper, we have investigated the response of commercial n-type SHJ cells to illuminated annealing under a broad range of illumination intensities (1–40 kWm^{-2}) and temperatures (25–180 °C). Firstly, we have presented results showing an increase in η of up to 0.3% absolute after dark annealing at 160 °C for 3 min, attributed to improved surface passivation and a reduction in R_S. Secondly, we identified a temperature-dependent LID mechanism at temperatures of 85 °C and above under 1-sun illumination (broadband halogen), with both the degradation extent and rate increasing with annealing temperature. At 160 °C, an average η loss of 0.5 ± 0.3% absolute was observed after only 5 min, and exceeding 0.8% in some cells. A subsequent recovery was observed with continued exposure to illumination, reducing the net η loss to 0.05 ± 0.1% absolute after 2 h at 160 °C.

An increase in cell temperature was found to result in accelerated kinetics of the initial degradation phase, and typically leads to a greater maximum extent of degradation for a given illumination intensity. An apparent threshold temperature was observed around 120 °C, below which the LID defect is not strongly activated (or the kinetics are sufficiently slow such that the cells are effectively stable over the timeframe investigated herein), even when exposed to extremely high illumination intensities (40 kWm^{-2}). However, when above this temperature threshold, increasing illumination intensity was found to strongly accelerate the kinetics of the subsequent recovery phase, while exhibiting no significant impact on the degradation phase.

Importantly, increasing the illumination intensity to 40 kWm^{-2} can result in a net η improvement of 0.2% absolute at 150 °C within 100 s. These results suggest that rapid enhancement of SHJ solar cell efficiency can be obtained using illuminated annealing at elevated temperatures,

however, these same processes can also be detrimental to cell performance if not carefully optimised. Additional studies are required to validate the long-term stability of such a process, as well as reduce processing times to make efficiency enhancements industrially feasible.

The underlying mechanism for the observed LID behaviour remains uncertain, however SWE type defect mobility in the a-Si:H interlayer and changes to hydrogen passivation (and even effusion) could account for the observed behaviour. Further studies are required to investigate the primary factors and causal mechanism(s) underlying the observed LID behaviour, and how best to avoid defect activation or achieve robust mitigation with illuminated annealing treatments.

CRediT authorship contribution statement

Chukwuka Madumelu: Conceptualization, Investigation, Writing - original draft. **Brendan Wright:** Conceptualization, Methodology, Investigation, Writing - original draft. **Anastasia Soeriyadi:** Investigation. **Matthew Wright:** Investigation. **Daniel Chen:** Investigation. **Bram Hoex:** Methodology, Writing - review & editing. **Brett Hallam:** Conceptualization, Methodology, Supervision, Funding acquisition, Writing - review & editing.

Declaration of competing interest

The authors declare that they have no known competing financial interests or personal relationships that could have appeared to influence the work reported in this paper.

Acknowledgements

This work was supported by the Australian Government through the Australian Renewable Energy Agency (ARENA: 2017/RND003, 2017/RND005). The views expressed herein are not necessarily the views of the Australian Government, and the Australian Government does not accept responsibility for any information or advice contained herein. Brett Hallam would like to acknowledge the support of the Australian Research Council (ARC) through a Discovery Early Career Researcher Award (DE170100620). The authors would like to thank Michael Pollard for his assistance with the set-up of the custom in-situ V_{OC} tool, and the entire team at the Solar Industrial Research Facility (SIRF) for provision of facilities and equipment used for characterisation.

References

[1] Mikio Taguchi, Ayumu Yano, Satoshi Tohoda, Kenta Matsuyama, Yuya Nakamura, Takeshi Nishiwaki, Kazunori Fujita, Eiji Maruyama, 24.7% record efficiency hit solar cell on thin silicon wafer, IEEE Journal of Photovoltaics 4 (1) (2014) 96–99.
[2] Kunta Yoshikawa, Hayato Kawasaki, Wataru Yoshida, Toru Irie, Katsunori Konishi, Kunihiro Nakano, Toshihiko Uto, Daisuke Adachi, Masanori Kanematsu, Hisashi Uzu, Kenji Yamamoto, Silicon heterojunction solar cell with interdigitated back contacts for a photoconversion efficiency over 26%, Nature Energy 2 (5) (2017).
[3] Mikio Taguchi, Eiji Maruyama, Makoto Tanaka, Temperature dependence of amorphous/crystalline silicon heterojunction solar cells, Jap. J. Appl. Phys. 47 (814) (2008).
[4] Bénédicte Demaurex, Passivating Contacts for Homojunction Solar Cells Using A-Si:h/c-Si Hetero-Interfaces, 2014, 6392:1–182.
[5] Haschke Jan, Olivier Dupré, Mathieu Boccard, Christophe Ballif, Silicon heterojunction solar cells: recent technological development and practical aspects - from lab to industry, Sol. Energy Mater. Sol. Cell. 187 (February) (2018) 140–153.
[6] Bandana Singha, Chetan S. Solanki, N-type solar cells: advantages, issues, and current scenarios, Sol. Energy Mater. Sol. Cell. 4 (2017), 072001.
[7] Itrpv, International Technology Roadmap for Photovoltaic (Itrpv), tenth ed., 2019, pp. 1–38. Itrpv.
[8] Dirk C. Jordan, Chris Deline, Steve Johnston, Steve R. Rummel, Bill Sekulic, Hacke Peter, Sarah R. Kurtz, Kristopher O. Davis, Eric John Schneller, Xingshu Sun, Muhammad A. Alam, Ronald A. Sinton, Silicon heterojunction system field performance, IEEE Journal of Photovoltaics 8 (1) (2018) 177–182.
[9] Vikrant Sharma, O.S. Sastry, Arun Kumar, Birinchi Bora, S.S. Chandel, Degradation analysis of a-si, (hit) hetro-junction intrinsic thin layer silicon and m-c-si solar photovoltaic technologies under outdoor conditions, Energy 72 (2014) 536–546.
[10] Joseph Karas, Archana Sinha, Viswa Sai Pavan Buddha, Fang Li, Farhad Moghadam, Govindasamy Tamizhmani, Stuart Bowden, André Augusto, Damp heat induced degradation of silicon heterojunction solar cells with cu-plated contacts, IEEE Journal of Photovoltaics 10 (1) (2020) 153–158.
[11] Taweewat Krajangsang, Shunsuke Kasashima, Aswin Hongsingthong, Porponth Sichanugrist, Makoto Konagai, Effect of p-μc-si1-xox:h layer on performance of hetero-junction microcrystalline silicon solar cells under light concentration, Curr. Appl. Phys. 12 (2) (2012) 515–520.
[12] Eiji Kobayashi, Stefaan De Wolf, Jacques Levrat, Gabriel Christmann, Descoeudres Antoine, Sylvain Nicolay, Matthieu Despeisse, Yoshimi Watabe, Christophe Ballif, Light-induced performance increase of silicon heterojunction solar cells, Appl. Phys. Lett. 109 (153503) (2016).
[13] Eiji Kobayashi, Stefaan De Wolf, Jacques Levrat, Antoine Descoeudres, Matthieu Despeisse, Franz Josef Haug, Christophe Ballif, Increasing the efficiency of silicon heterojunction solar cells and modules by light soaking, Sol. Energy Mater. Sol. Cell. 173 (March) (2017) 43–49.
[14] Pratish Mahtani, Varache Renaud, Bastien Jovet, Christophe Longeaud, Jean Paul Kleider, Nazir P. Kherani, Light induced changes in the amorphous - crystalline silicon heterointerface, J. Appl. Phys. 114 (12) (2013).
[15] Stefaan De Wolf, Benedicte Demaurex, Descoeudres Antoine, Christophe Ballif, Very fast light-induced degradation of a-si:h/c-si(100) interfaces, Phys. Rev. B 83 (233301) (2011).
[16] Simone Bernardini, Mariana I. Bertoni, Insights into the degradation of amorphous silicon passivation layer for heterojunction solar cells, Physica Status Solidi (A) Applications and Materials Science 216 (4) (2019) 1–6.
[17] D.L. Staebler, C.R. Wronski, Reversible conductivity changes indischarge-produced amorphous si, Appl. Phys. Lett. 31 (292) (1977).
[18] Ihsanul Afdi Yunaz, Kenji Hashizume, Shinsuke Miyajima, Akira Yamada, Makoto Konagai, Fabrication of amorphous silicon carbide films using vhf-pecvd for triple-junction thin-film solar cell applications, Sol. Energy Mater. Sol. Cell. 93 (6–7) (2009) 1056–1061.
[19] Sorapong Inthisang, Kobsak Sriprapha, Shinsuke Miyajima, Akira Yamada, Makoto Konagai, Hydrogenated amorphous silicon oxide solar cells fabricated near the phase transition between amorphous and microcrystalline structures, Jpn. J. Appl. Phys. 48 (12) (2009).
[20] Tatsuo Shimizu, Staebler-wronski effect in hydrogenated amorphous silicon and related alloy films, Jpn. J. Appl. Phys., Part 1: Regular Papers and Short Notes and Review Papers 43 (6 A) (2004) 3257–3268.
[21] H. Dersch, J. Stuke, J. Beichler, Light-induced dangling bonds in hydrogenated amorphous silicon, Appl. Phys. Lett. 38 (6) (1981) 456–458.
[22] M. Stutzmann, W.B. Jackson, C.C. Tsai, Light-induced metastable defects in hydrogenated amorphous silicon: a systematic study, Phys. Rev. B 32 (23) (1985).
[23] Michio Ohsawa, Toshio Hama, Toshiaki Akasaka, Takeshige Ichimura, Hiroshi Sakai, Sueshige Ishida, Yoshiyuki Uchida, The role of hydrogen in the staebler-wronski effect of a-si:h. Japanese, J. Appl. Phys. 24 (10) (1985) L838–L840.
[24] K. Petter, K. Hubener, F. Kersten, M. Bartzsch, F. Fertig, B. Kloter, J. Muller, Dependence of letid on brick height for different wafer suppliers with several resistivities and dopants, 9th Int. Work. Cryst. Silicon Sol. Cells 6 (1) (2016).
[25] Friederike Kersten, Peter Engelhart, Hans Christoph Ploigt, Andrey Stekolnikov, Thomas Lindner, Florian Stenzel, Matthias Bartzsch, Andy Szpeth, Kai Petter, Johannes Heitmann, Jorg W. Muller, A new mc-si degradation effect called letid, in: IEEE 42nd Photovoltaic Specialist Conference vol 2015, PVSC, 2015, p. 2015.
[26] Fabian Fertig, Karin Krauß, Stefan Rein, Light-induced degradation of pecvd aluminium oxide passivated silicon solar cells, Phys. Status Solidi Rapid Res. Lett. 9 (1) (2015) 41–46.
[27] K. Ramspeck, S. Zimmermann, H. Nagel, A. Metz, Y. Gassenbauer, B. Birkmann, A. Seidl, Light Induced Degradation of Rear Passivated Mc-Si Solar Cells, vol 53, 2012, pp. 1689–1699.
[28] Daniel Chen, Phillip G. Hamer, Moonyong Kim, Tsun H. Fung, Gabrielle Bourret-Sicotte, Shaoyang Liu, Catherine E. Chan, Alison Ciesla, Ran Chen, Malcolm D. Abbott, Brett J. Hallam, Stuart R. Wenham, Hydrogen induced degradation: a possible mechanism for light- and elevated temperature- induced degradation in n-type silicon, Sol. Energy Mater. Sol. Cell. 185 (May) (2018) 174–182.
[29] Tim Niewelt, Regina Post, Florian Schindler, Wolfram Kwapil, C. Martin, Schubert, Investigation of letid where we can control it - application of fz silicon for defect studies, AIP Conference Proceedings 2147 (2019), 140006.
[30] M.A. Jensen, A. Zuschlag, S. Wieghold, D. Skorka, A.E. Morishige, G. Hahn, T. Buonassisi, Evaluating root cause: the distinct roles of hydrogen and firing in activating light- a nd elevated temperature-induced degradation, J. Appl. Phys. 124 (8) (2018).
[31] Alison Ciesla Nee Wenham, Wenham Stuart, Ran Chen, Catherine Chan, Daniel Chen, Brett Hallam, David Payne, Tsun Fung, Moonyong Kim, Shaoyang Liu, Sisi Wang, Kyung Kim, Aref Samadi, Chandany Sen, Carlos Vargas, Utkarshaa Varshney, Bruno Vicari Stefani, Phillip Hamer, Gabrielle Bourret-Sicotte, Nitin Nampalli, Ziv Hameiri, Cheemun Chong, Malcolm Abbott, Hydrogen-induced degradation, in: 2018 IEEE 7th World Conference on Photovoltaic Energy Conversion, WCPEC 2018 - A Joint Conference of 45th IEEE PVSC, 28th PVSEC and 34th EU PVSEC, 2018, pp. 1–8.
[32] Utkarshaa Varshney, Malcolm Abbott, Alison Ciesla, Daniel Chen, Shaoyang Liu, Chandany Sen, Moonyong Kim, Wenham Stuart, Bram Hoex, Catherine Chan, Evaluating the impact of sinx thickness on lifetime degradation in silicon, IEEE Journal of Photovoltaics 9 (3) (2019) 601–607.
[33] Catherine Chan, Tsun Hang Fung, Malcolm Abbott, David Payne, Alison Wenham, Brett Hallam, Ran Chen, Wenham Stuart, Modulation of carrier-induced defect

kinetics in multi-crystalline silicon perc cells through dark annealing, Solar RRL 1 (2) (2017) 1600028.
[34] Kenta Nakayashiki, Jasmin Hofstetter, Ashley E. Morishige, Tsu-Tsung Andrew Li, David Berney Needleman, Mallory A. Jensen, Tonio Buonassisi, Engineering solutions and root-cause analysis for light-induced degradation in p-type multicrystalline silicon perc modules, IEEE JOURNAL OF PHOTOVOLTAICS 6 (860) (2016).
[35] Catherine E. Chan, David N.R. Payne, Brett J. Hallam, Malcolm D. Abbott, Tsun H. Fung, Alison M. Wenham, Budi S. Tjahjono, Stuart R. Wenham, Rapid stabilization of high-performance multicrystalline p-type silicon perc cells, IEEE JOURNAL OF PHOTOVOLTAICS 6 (1473) (2016).
[36] Dennis Bredemeier, Dominic Walter, Sandra Herlufsen, Jan Schmidt, Lifetime degradation and regeneration in multicrystalline silicon under illumination at elevated temperature, AIP Adv. 6 (2016), 035119.
[37] David Sperber, Florian Furtwängler, Axel Herguth, Giso Hahn, Does letid occur in c-si even without a firing step? AIP Conf. Proc. 2147 (1) (2019) 140011. AIP Publishing LLC.
[38] Bruno Vicari Stefani, et al., Large-area Boron-Doped 1.6 Ωcm P-type Czochralski Silicon Heterojunction Solar Cells with a Stable Open-Circuit Voltage of 736 Mv and Efficiency of 22.0%, Solar RRL, 2020. Press.
[39] Chang Sun, Daniel Chen, Fiacre Rougieux, Rabin Basnet, Brett Hallam, Daniel Macdonald, Kinetics and dynamics of the regeneration of boron-oxygen defects incompensated n-type silicon, Sol. Energy Mater. Sol. Cell. 195 (174) (2019).
[40] Martin Wolf, Hans Rauschenbach, Series resistance effects on solar cell measurements, Adv. Energy Convers. 3 (2) (1963) 455–479.
[41] Daisuke Adachi, Jose Luis Hernandez, Kenji Yamamoto, Impact of carrier recombination on fill factor for large area heterojunctioncrystalline silicon solar cell with 25.1% efficiency, Appl. Phys. Lett. 107 (233506) (2015).
[42] Brett J. Hallam, Phill G. Hamer, Sisi Wang, Lihui Song, Nitin Nampalli, Malcolm D. Abbott, Catherine E. Chan, Doris Lu, Alison M. Wenham, Ly Mai, Nino Borojevic, Alex Li, Daniel Chen, Moon Yong Kim, Azmeer Azmi, Wenham Stuart, Advanced hydrogenation of dislocation clusters and boron-oxygen defects in silicon solar cells, Energy Procedia 77 (799) (2015).
[43] Sopori Bhushan, Basnyat Prakash, Devayajanam Srinivas, Sudhakar Shet, Vishal Mehta, Jeff Binns, Jesse Appel, Understanding Light-Induced Degradation of C-Si Solar Cells, IEEE, 2011, 001115.
[44] Heiko Steinkemper, Hermle Martin, Stefan W. Glunz, Comprehensive simulation study of industrially relevant silicon solar cell architectures for an optimal material parameter choice, Prog. Photovoltaics Res. Appl. 24 (10) (2016) 1319–1331.
[45] J. Kakalios, R.A. Street, W.B. Jackson, Stretched-exponential relaxation arising from dispersive diffusion of hydrogen in amorphous silicon, Phys. Rev. Lett. 59 (1037) (1987).
[46] B.W. Clare, J.C.L. Cornish, G.T. Hefter, P.J. Jennings, C.P. Lund, D.J. Santjojo, M.O. G. Talukder, Studies of photodegradation in hydrogenated amorphous silicon, Thin Solid Films 288 (76) (1996).
[47] Stefaan De Wolf, Sara Olibet, Christophe Ballif, Stretched-exponential a-si:h/c-si interface recombination decay, J. Appl. Phys. Lett. 93 (2008), 032101.
[48] Pratish Mahtani, Varache Renaud, Bastien Jovet, Christophe Longeaud, Jean-Paul Kleider, Nazir P. Kherani, Light induced changes in the amorphous-crystalline silicon heterointerface, J. Appl. Phys. 114 (124503) (2013).
[49] El Mahdi El Mhamdi, Jakub Holovsky, Benedicte Demaurex, Christophe Ballif, Stefaan De Wolf, Is light-induced degradation of a-si:h/c-si interfaces reversible? Appl. Phys. Lett. 104 (252108) (2014).